2013 European Control Conference (ECC)
July 17-19, 2013, Zürich, Switzerland.

Fault Tolerant Control for Polynomial Linear Parameter Varying (LPV) Systems applied to the stabilization of a riderless bicycle

J. A. Brizuela-Mendoza[1], C. M. Astorga-Zaragoza[1], A. Zavala-Río[2], F. Canales-Abarca[3] and J. Reyes-Reyes[1]

***Abstract*— This paper presents the results of a Fault Tolerant Control based on observers for polynomial LPV systems. The main contribution lies in observers, controller, Fault Diagnosis and Isolation unit and Fault Tolerant Control (FTC) design procedure, based on the solution of Parameterized Linear Matrix Inequalities (PLMI) with application to a riderless bicycle dynamics. Further, unlike previous works, this approach takes for its design only the measured outputs provided by the in-built bicycle prototype sensors, eliminating the necessity of additional computations for the control law. The previous fact is viewed as an additional contribution in this development.**

I. INTRODUCTION

The bicycle dynamics has been, recently, an important topic in control research area. Several studies have been developed mainly referred to control systems that allow, through bicycle's handlebars manipulations and the velocity of the rear wheel, the tracking of defined paths [8] or the bicycle's balance. By using non-linear controllers and additional elements named balancers, [9][10] achieve the bicycle's stabilization and [11], taking a torque for the maneuver and rear wheel as input forces, meets the control objectives previously mentioned. In [12], sliding mode control theory has been applied for this dynamics and finally fuzzy controls for roll angle tracking can be found in [13]. While these papers apply to the study case, they reach the objective by taking the bicycle within defined trajectories or velocities. However, the works reported in [14] and [3] use dynamics models incorporating the vehicle speed. Under this condition, the prototype does not have a rear wheel system traction, becoming the control objective to maintain the upright position of the bicycle despite of the decreasing speed. In FTC framework, on the other hand, there are no works reported under this specific dynamical conditions. As a result, this issue is considered one of the main contributions in this paper. The efficiency of the proposed FTC scheme is shown with two numeric simulations, considering sensor's faults such as absence and loss of effectiveness.

II. RIDERLESS BICYCLE DYNAMICS

According to [1][2] the bicycle dynamics could be represented by the decomposition of the system in four bodies, a general framework which includes a rigid body (rider), a front frame composed by the handle and, each tire. Degrees of freedom are adopted referring to the roll angle $\phi(t)$ with respect to the horizontal, the steer angle $\delta(t)$ of the front frame and, the bicycle speed $v(t)$, taking as input forces a torque applied to the steer $T_\delta(t)$ and roll angle $T_\phi(t)$.

$$G\ddot{q}(t) + v(t)C_1\dot{q}(t) + (gK_0 + v^2(t)K_1)q(t) = f(t) \quad (1)$$

$$q = \begin{bmatrix} \phi(t) \\ \delta(t) \end{bmatrix} \quad f(t) = \begin{bmatrix} T_\phi(t) \\ T_\delta(t) \end{bmatrix} \quad (2)$$

where G, C_1, K_0 and K_1 correspond to constant values dependent on the physics of the prototype and g is taken as gravity actions. Defining $x(t) = \begin{bmatrix}\phi(t)\ \delta(t)\ \dot{\phi}(t)\ \dot{\delta}(t)\end{bmatrix}'$ and taking $T_\delta(t)$ as a unique input force, the space state representation is obtained for the dynamic system in subject.

$$\begin{aligned} \dot{x}(t) &= A(v(t))x(t) + Bu(t) \\ y(t) &= Cx(t) \end{aligned} \quad (3)$$

From (3) it is possible to see a parametric dependence in $v(t)$ which qualifies this model as LPV system. Further, due to the $v^2(t)$ term in (1), we have a polynomial influence in the system matrix $A(v(t))$. Using the physics values presented in [14] [3], we have the data for (3) according to the following equations.

$$A(v) = \begin{bmatrix} 0 & 0 & 1 & 0 \\ 0 & 0 & 0 & 1 \\ 13.67 & 0.225 - 1.319v^2 & -0.164v & -0.552v \\ 4.857 & 10.81 - 1.125v^2 & 3.621v & -2.388v \end{bmatrix} \quad (4)$$

$$B = \begin{bmatrix} 0 \\ 0 \\ -0.339 \\ 7.457 \end{bmatrix} \quad (5)$$

From now on we eliminate the term (t) for practical reasons by defining $v := v(t)$, as well as for x, y, u, e, and η. Based on [14] [3], there are only two measured outputs: the position for steer angle δ and the velocity of the roll angle $\dot{\phi}$, consequently, the output matrix C for (3) acquires the following representation.

$$C = \begin{bmatrix} C_1 \\ C_2 \end{bmatrix} = \begin{bmatrix} 0 & 1 & 0 & 0 \\ 0 & 0 & 1 & 0 \end{bmatrix} \quad (6)$$

Previous works use, for control purposes, additional operations related to filtered differentiation and numeric integration in order to have $y = x$ from the available measurements, unlike the results presented in this paper.

[1]Electronics Engineering Department, National Center for Research and Technological Development (cenidet), Cuernavaca,Mex.
[2]Applied Mathematics Department, Potosino Institute of Scientific and Technological Research (IPICYT), SLP.,Mex.
[3]ABB Corporate Research, Switzerland.

III. Riderless Bicycle System Controllability, Observability and Stability Conditions

The controllability and observability conditions for a dynamic system represents an important criteria to analyze before the controller's or observer's design and, for LPV systems, these can be seen as an extension for LTI systems. Due to the dependency in the parameter varying v, it is necessary to know those values which cause a loss of any of these conditions. By making:

$$|\Lambda_c| = |[B \;\; A(v)B \;\; A(v)^2B \;\; A(v)^3B]| = 0$$

$$|\Lambda_c| = -5806.5321v^4 + 19463.1274v^2 - 22.3115 = 0 \quad (7)$$

and solving for v (where $|*|$ stands for determinant operation), we find the values of controllability loss in the following set.

$$v_c = \{\pm 1.8305168, \pm 0.033863576\} \quad (8)$$

Meanwhile, the observability condition is not achieve when v acquires values such that:

$$|\Lambda_{oi}| = |[C_i \;\; C_iA(v) \;\; C_iA(v)^2 \;\; C_iA(v)^3]'| = 0 \quad i = 1, 2$$

where $C = [C_1 \;\; C_2]'$. With C_1:

$$|\Lambda_{o1}| = -182.1204v^2 - 23.5904 = 0 \quad (10)$$

and yields the next set of values for v.

$$v_{o1} = \{\pm 0.35991\} \quad (11)$$

Using C_2, we obtain:

$$|\Lambda_{o2}| = 3.0854v^6 - 82.6582v^4 + 527.1539v^2 - 7.4256 = 0 \quad (12)$$

with the values for v according to (13).

$$v_{o2} = \{\pm 4.04326, \pm 3.22923, \pm 0.11882\} \quad (13)$$

In other words, if v coincides with any of the elements expressed in (8), (11), and (13), then the riderless bicycle system (3) will present a loss of controllability and/or observability conditions. For this reason our operation region is defined in $\Omega := \{v|\ 0.5(m/sec) \leq v \leq 1.8(m/sec)\}$, under the consideration that, within this range, the system is unstable (Fig. 1) but suitable to be controlled and observed.

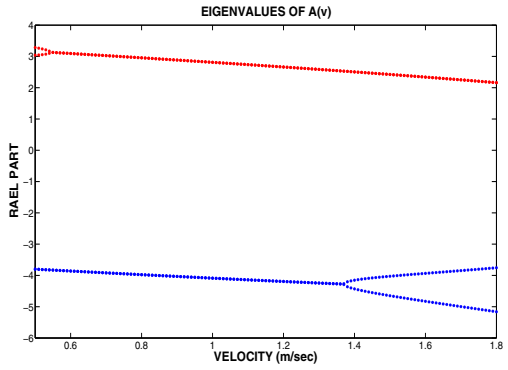

Fig. 1. Open-Loop Eigenvalues

IV. Control System Description for the Riderless Bicycle Dynamics

The purpose of control is to maintain the up-right position of the bicycle despite of the vehicle's speed. Having only two measured signals $\dot{\phi}$ and δ, we propose a control law:

$$u = k(v)\hat{x} \quad (14)$$

with $\hat{x}$ been the estimated of x.

A. Observer design

For the observer design we use and observer with the following structure:

$$\dot{\hat{x}} = A(v)\hat{x} + Bu + L(v)(y - \hat{y}) \quad (15)$$

Making the estimation error $e = x - \hat{x}$, we reach the well known dynamical equation for estimation error:

$$\dot{e} = (A(v) - L(v)C)e \quad (16)$$

The objective is to determine $L(v)$ such $e \to 0$ as $t \to \infty \; \forall \; v \in \Omega$. We begin with the stability for LPV systems by using a Lyapunov function $V(v, e) = e^{'}P(v)e$ ($P(v)$ depending on v in order to meet the condition of $A(v)$) according to [4] :

$$P(v)H(v) + H(v)'P(v) + \rho\frac{\partial P(v)}{\partial t} < 0$$
$$P(v) = P(v)' > 0 \;\; \forall \, v \in \Omega \quad (17)$$

Taking $C = [C_1 \;\; C_2]'$, $L(v) = [L_1(v) \;\; L_2(v)]$, $H(v) = A(v) - L_1(v)C_1 - L_2(v)C_2$ and removing the bilinearity resulting by replacing $X_1(v) = P(v)L_1(v)$ and $X_2(v) = P(v)L_2(v)$ the following can be obtained.

$$\begin{gathered} P(v)A(v) - X_1(v)C_1 - X_2(v)C_2 + \\ A(v)'P(v) - C_1'X_1(v)' - C_2'X_2(v)' + \\ \rho\frac{\partial P(v)}{\partial t} < 0 \end{gathered}$$
$$P(v) = P(v)' > 0 \;\; \forall \, v \in \Omega \quad (18)$$

Finally the observer gain should be computed by:

$$\begin{gathered} X_i(v) = P(v)L_i(v) \\ L_i(v)' = X_i(v)'(P(v))^{-1} \;\; i = 1, 2. \end{gathered} \quad (19)$$

It is included, for better results, an LMI region [5] such that:

$$\begin{gathered} P(v)A(v) - X_1(v)C_1 - X_2(v)C_2 + \\ A(v)'P(v) - C_1'X_1(v)' - C_2'X_2(v)' + \\ P(v)2\alpha < 0 \;\; \forall \, v \in \Omega \end{gathered} \quad (20)$$

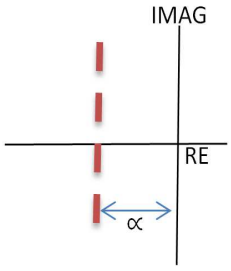

Fig. 2. LMI Region

B. Controller Design

By making the closed-loop system $H(v) = A(v) + Bk(v)$ and replacing it in (17), (21) can be computed.

$$P(v)(A(v) + Bk(v)) + (A(v) + Bk(v))'P(v) + \rho\frac{\partial P(v)}{\partial t} < 0$$
$$P(v) = P(v)' > 0 \quad \forall\, v \in \Omega \tag{21}$$

Pre-multiplying and post-multiplying by $P(v)^{-1}$ and naming $Y(v) = P(v)^{-1}$, $E(v) = k(v)Y(v)$:

$$A(v)Y(v) + BE(v) + Y(v)'A(v)' + E(v)'B' - \rho\frac{\partial Y(v)}{\partial t} < 0$$
$$Y(v) = Y(v)' > 0 \quad \forall\, v \in \Omega \tag{22}$$

The control gains will be determined by (23).

$$k(v) = E(v)Y(v)^{-1} \tag{23}$$

As in the observer design, we use a LMI region such that:

$$A(v)Y(v) + BE(v) + Y(v)'A(v)' + E(v)'B' + 2\alpha Y(v) < 0 \quad \forall\, v \in \Omega \tag{24}$$

C. Solution procedure for controller and observer

The LMI set in previous sections can be seen as a set of linear matrix inequalities parameterized in time through de parameter varying v. The methods for solving these problems found in the literature are relaxation [6], Sum of the Squares [7], and gridding techniques [5]. This approach uses the last one of these, which is based on a discretization for the parameter varying space using a difference approximation for the derivative term. Once this has been done, an interpolation method is used for making the solution continuous. The final LMI set to be solved for the observer will be:

$$\begin{gathered} P(jh)A(jh) - X_1(jh)C_1 - X_2(jh)C_2 + A(jh)'P(jh) \\ -C_1'X_1(jh)' - C_2'X_2(jh)' \pm \rho\frac{P(jh+h) - P(jh)}{h} < 0 \\ P(jh)A(jh) - X_1(jh)C_1 - X_2(jh)C_2 + A(jh)'P(jh) \\ -C_1'X_1(jh)' - C_2'X_2(jh)' + P(jh)2\alpha < 0 \\ P(jh) = P(jh)' > 0 \;\; \forall \;\; jh \in \Omega \end{gathered} \tag{25}$$

And for control:

$$\begin{gathered} A(jh)Y(jh) + BE(jh) + Y'(jh)A(jh)' + E(jh)'TB' \\ \pm\rho\frac{Y(jh+h) - Y(jh)}{h} < 0 \\ A(jh)Y(jh) + BE(jh) + Y'(jh)A(jh)^T + E(jh)'TB' \\ +2\alpha Y(jh) < 0 \\ Y(jh) = Y(jh)' > 0 \;\; \forall \;\; jh \in \Omega \end{gathered} \tag{26}$$

Where $j = 1, 2, ..., N$ is the gridding parameter varying space and $h > 0$ the step width. (25) and (26) were solved using MATLAB and Yalmip [16] numeric solver.

V. Controlled system: Free Fault case

It is defined the gridding parameter varying space with $N = 52$, width $h = 0.025$ and $\rho = 0.05$. Further, we use a LMI region for observer purposes $\alpha = 5$ and a LMI region $\alpha = 1.2$ for the controller. The final observer gains can be seen in Fig. 3 by using functions of 7th order for each element of $L_{i\sigma}(v), i = 1, 2$ and $\sigma = 1, 2, ..., 4$.

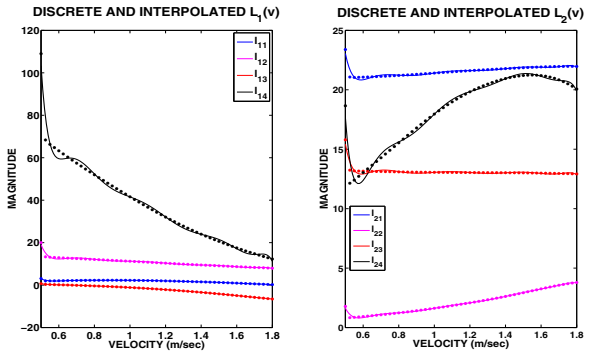

Fig. 3. $L_{i\sigma}$(v) Gains

Meanwhile, the computed controller gains are presented in Fig. 4 using interpolated functions of 9th order for each element of $k_\sigma(v)$.

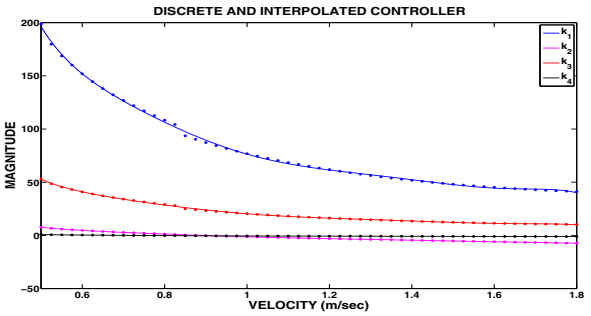

Fig. 4. $k_\sigma(v)$ Gains

By making the closed-loop system matrix (27) and obtaining its eigenvalues (Fig. 5):

$$\begin{bmatrix} \dot{x} \\ \dot{e} \end{bmatrix} = \begin{bmatrix} A(v) + Bk(v) & -Bk(v) \\ 0 & A(v) - L(v)C \end{bmatrix} \begin{bmatrix} x \\ e \end{bmatrix} \tag{27}$$

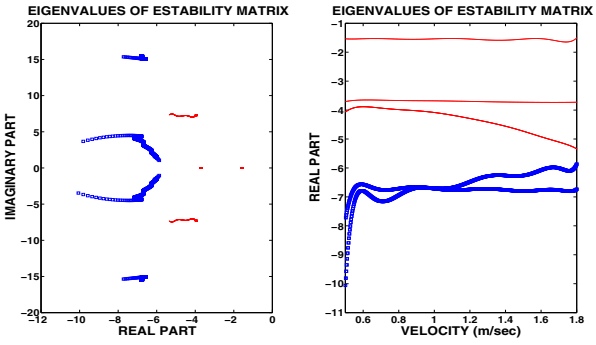

Fig. 5. Closed-Loop System Eigenvalues

From Fig. 5 it can be seen the eigenvalues corresponding to $A(v) - L(v)C$ (thick set), while the rest will be for $A(v) + Bk(v)$. Finally, Fig. 6 presents the results for the controlled system and estimation error for the observer, from initial conditions $x = [-2.25 \quad 0 \quad 0.2 \quad 0]'$ and $\hat{x} = [-1.8 \quad -0.35 \quad 0.85 \quad -0.2]'$.

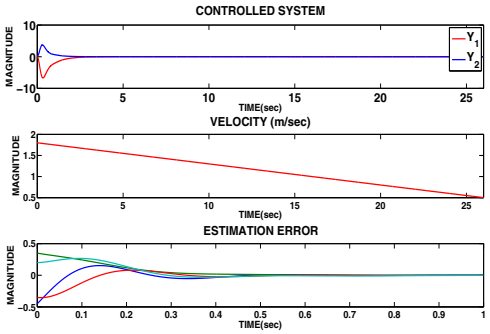

Fig. 6. Controlled System Free Fault Case

VI. Riderless Bicycle Proposal FTC scheme

The proposal of this work is to take only the measurements available for control purposes and detect the faults in their corresponding sensors. In the faulty condition of the output sensor for Y_1 , u will be constructed by $\hat{x}$ through a non-faulty estimation observer using the output Y_2 and, in the opposite faulty case, u will take $\hat{x}$ from Y_1 (Fig. 7). For the fault in δ sensor, the observer gains $L_{2f}(v)$ will be designed with $\alpha = 0.1$ using functions of 3,10,2 and 10th order for each σ element, while in case of fault in $\dot{\phi}$ sensor, $L_{1f}(v)$ uses $\alpha = 1.2$ and functions of 4,1,7 and 6th order.

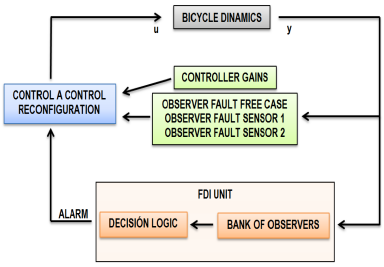

Fig. 7. FTC Scheme

This paper's results use an FDI observer based on a Dedicated Observer Scheme [15]. Under this approach, there are two observers in charge of the residual generation $L_{1fdi}(v)$ and $L_{2fdi}(v)$, both use the input $u = k(v)\hat{x}$ and will be driven for each output of the system (see Fig. 8). With this in mind, there are 4 elements in the residual named $R_{11}, R_{12}, R_{21}, R_{22}$, which must be evaluated in a decision logic unit in order to detect and isolate the fault. This unit produces an alarm indication correspondent from a loss of effectiveness of 5 % to complete absence of δ sensor and a loss of effectiveness of 40 % to complete absence for $\dot{\phi}$ sensor.

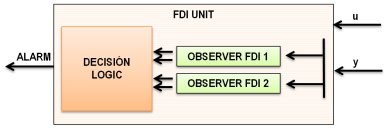

Fig. 8. FDI Unit

All the observer's gains for the FDI unit ($L_{1fdi}(v)$ and $L_{2fdi}(v)$ and for faulty system condition ($L_{1f}(v)$ and $L_{2f}(v)$) will be performed by the same procedure detailed in previous sections.

The final observers for FDI purposes L_{1fdi} and L_{2fdi} were designed:

- L_{1fdi}, $\alpha = 0.5$, interpolated functions of 10,6,6 and 6th order, respectively.
- L_{2fdi}, $\alpha = 2$, interpolated functions of 8,10,2 and 10th order, respectively.

By making the residual analysis, the decision logic unit produces faulty alarms based on the following statements:

- If $R_{12} < -2$ then $\dot{\phi}$ sensor fault and alarm=1.
- If $R_{21} < 8^{-3}$ and $R_{12} > -1.8$ then δ sensor fault and alarm=2.

VII. Riderless Bicycle FTC simulations results

The following corresponds to the main results for the proposal FTC scheme, remembering that, under faulty condition, the system output can be represented by:

$$y = Cx + C\eta \tag{28}$$

been $\eta = [0 \;\; f_1 \;\; f_2 \;\; 0]'$. Three scenarios will be taken in consideration:

- Absence of δ sensor at t=5 sec, $f_1 = -1$.
- Absence of $\dot{\phi}$ sensor at t=6.5 sec, $f_2 = -1$
- Effectiveness loss in $\dot{\phi}$ sensor of 10% at t=7.2 sec, $f_2 = -0.1$.

A. Absence of δ sensor

From Fig. 9, it is possible to see the sensor fault occurrence and its correct reconfiguration. The first two plots show the faulty (dotted line) and reconfigured output 1 and output 2. The remaining plot shows the fault magnitude (continuous line for δ sensor and thicker continuous line for $\dot{\phi}$ sensor), alarm (dash-dot line) and variation of the parameter v (dashed line).

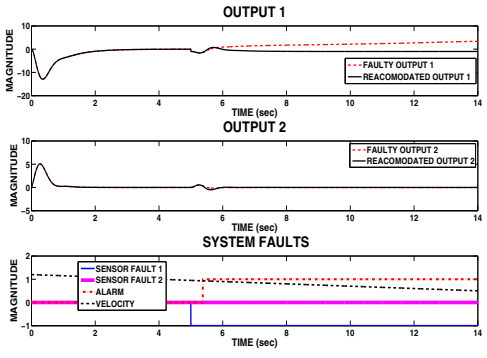

Fig. 9. Absense of δ sensor at t=5 sec.

The top plot of Fig. 10 shows the faulty (dotted line) and reconfigured control law using a variation for v from 1.2 to 0.5 (m/sec). Finally, Fig. 11 presents the residual generated by the fault. It is shown that the decision logic unit works correctly according to the values defined in section VI.

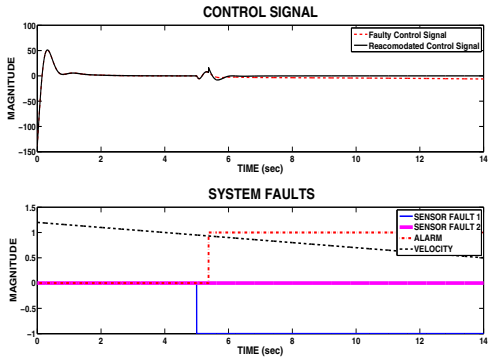

Fig. 10. Control law reconfiguration in absence of δ sensor at t=5 sec.

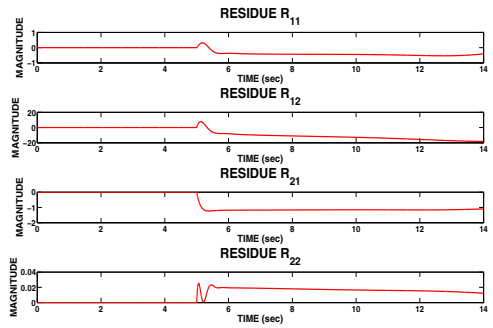

Fig. 11. Residual generated in absence of δ sensor at t=5 sec.

B. Absence of $\dot{\phi}$ sensor

Unlike the previous test, we present the results for absence $\dot{\phi}$ sensor using a variation for v from 1.7 to 1 (m/sec). The plot interpretation has the same description as in absence of δ sensor.

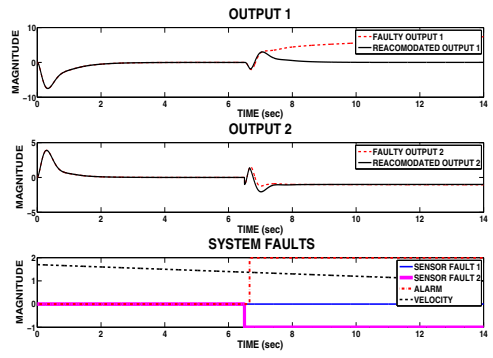

Fig. 12. Absence of $\dot{\phi}$ sensor at t=6.5 sec.

We can see, from Fig. 13, a greater effort for the control signal. This is caused for the influence of the roll angle (ϕ) liberty grade. In others words, the bicycle is more susceptible to this kind of fault than the one occurred for δ. The residual generated, meanwhile, corresponds to the presented in Fig. 14.

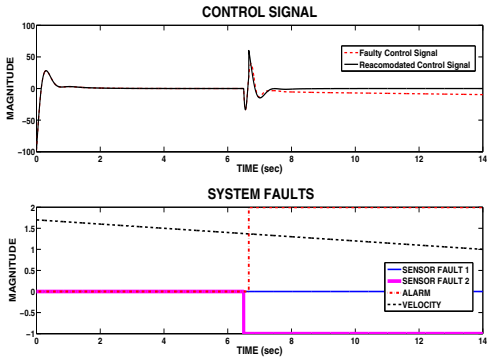

Fig. 13. Control law reconfiguration in absence of $\dot{\phi}$ sensor at t=6.5 sec.

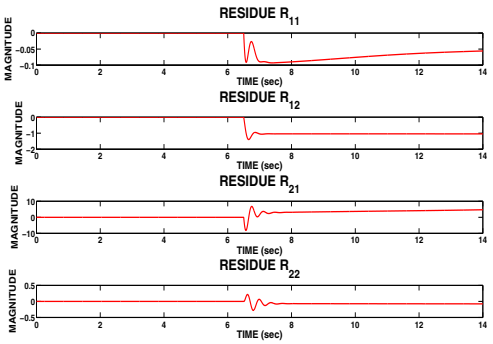

Fig. 14. Residual generated in absence of $\dot{\phi}$ sensor at t=6.5 sec.

C. Effectiveness loss in $\dot{\phi}$ sensor

Finally, we present the results for 10% effectiveness lost in $\dot{\phi}$ sensor at t=7.2 sec. This test, using a variation for v from 1.4 to 0.7 (m/sec), shows the proposal FTC efficiency for faults with minor magnitudes. Equally, Fig. 15 presents the system outputs and Fig. 16 contains the faulty and reconfigured control law.

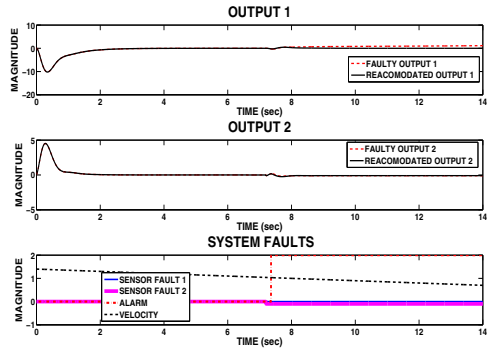

Fig. 15. Effectiveness loss in $\dot{\phi}$ sensor at t=7.2 sec.

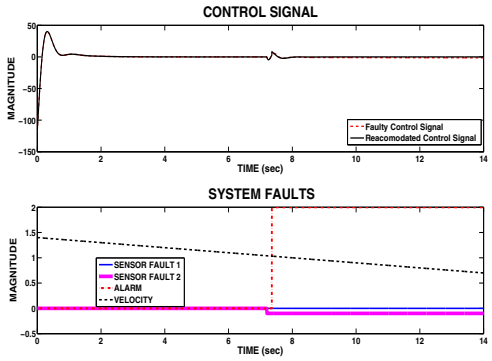

Fig. 16. Control law reconfiguration in Effectiveness loss of $\dot{\phi}$ sensor at t=7.2 sec.

The correct operation of FDI unit, despite the fault magnitude, is shown in Fig. 17.

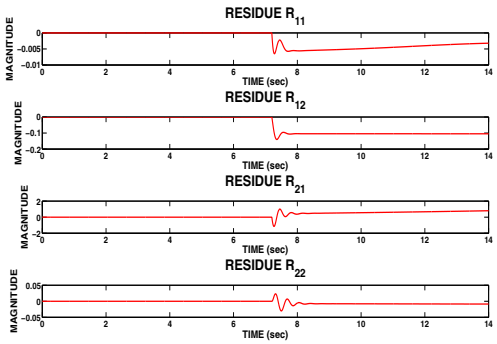

Fig. 17. Residual generated in Effectiveness loss of $\dot{\phi}$ sensor at t=7.2 sec.

VIII. CONCLUSIONS

From the simulation results shown, it is determined the correct operation of the FDI and the FTC proposal scheme, which conclude with the possibility to build a functional control system to solve faulty conditions in sensors in a LPV polynomial system. From the test carried out, the FTC has been successfully proved within all the operation regime described in section III, considering that the proposed scheme could be applied to a real prototype.

An important issue corresponds to the FDI unit. This work deals with absence or effectiveness loss in sensors but, under a BIAS faulty conditions; some troubles may appear due to the residual mechanism used. Future works will considered fault detection filters for FDI purposes. Despite the previous condition, this approach is taken as a starting point in the development of FTC in LPV polynomial systems.

ACKNOWLEDGMENT

To the National Council for Science and Technology (CONACYT) in Mexico. The first author was partially supported by IPICYT, Mexico.

REFERENCES

[1] A. Schwab, J. Meijaard, and J. Papadopoulos. A multibody dynamics benchmark on the equations of motion of an uncontrolled bicycle. in Proc. 5th EUROMECH Nonlinear Dynamics Conf. The Netherlands: Eindhoven Univ. Technol., Aug. 712, 2005, pp. 511-521.

[2] A. L. Schwab, J. P. Meijaard, J. M. Papadopoulos. Benchmark results on the linearized equations of motion of an uncontrolled bicycle. International Journal of Mechanical Science and Technology. 19(1), 2005, pp. 292-304.

[3] Vito Cerone, Davide Andreo, Mats Larsson and Diego Regruto. Stabilization of a Riderless Bicycle a Linear-Parameter-Varying Approach. Control Systems, IEEE. 30(5), 2010, pp. 23-32.

[4] Wilson J. Rugh, Jeff S. Shamma. Research on Gain Schedulling. Automatica 36, 2000, pp. 1401-1425.

[5] Mahmoud Chilali and Pascal Gahinet. H_∞ Design with Pole Placement Constraints: An LMI approach. IEEE Trans. on Automatic Control. 41(3), 1996, pp. 358-367.

[6] Pierre Apkarian and Hoang Duong Tuan. Parameterized LMI's in control theory. SIAM J. Control Optim. 38(4), 2000, pp. 1241-1264.

[7] S. Prajna and F. Wu. SOS-based solution approach to polynomial LPV system analysis and synthesis problems. International Journal on Control, 78, 2005, pp. 600-611.

[8] Getz, N.H. and Marsden. Control for an autonomous bicycle. J.E. Robotics and Automation. 1995 IEEE International Conference on, 1995, pp. 1397 - 1402.

[9] Lychek Keo and Masaki Yamakita. Controller design of an autonomous bicycle with both steering and balancer controls. In IEEE Multi-conference on Systems and Control, 2009.

[10] Masaki Yamakita and Atsuo Utano. Automatic control of bicycles with a balancer. In International Conference on Advanced Intelligent Mechatronics, 2005.

[11] Lei Guo, Qizheng Liao, Shimin Wei and Yonghua Huang. A kind of bicycle robot dynamic modeling and nonlinear control. Information and Automation (ICIA), 2010 IEEE International Conference on. pp. 1613 - 1617.

[12] Wen-Shyong Yu and Chan-Chih Yeh. Steering and balance controls of an electrical bicycle using integral sliding mode control. In International Conference on Robotics and Automation, 2011.

[13] Chih-Keng Chen and Thanh-Son Dao. Fuzzy control for equilibrium and roll-angle tracking of an unmanned bicycle. Multibody System Dynamics, 15(4), 2006, pp. 321-346.

[14] D. Dzung, D. Regruto, D. Andreo and V. Cerone. Experimental results on LPV stabilization of a riderless bicycle. In American Control Conference, 2009.

[15] Jie Chen and Ron. J Patton. Robust Model-Based Fault Diagnosis for Dynamics Systems. Kluwer Academic Publishers.

[16] Lab. of Autom. Control, Eidgenossische Tech. Hochschule, Zurich. YALMIP : a toolbox for modeling and optimization in MATLAB. IEEE International Symposium on Computer Aided Control Systems Design, 2004, pp. 284-289.